

# AAV vector based neonatal desensitization for the assessment of cell-replacement therapy for Parkinson's disease

---

Pavičić, Iva

Master's thesis / Diplomski rad

2021

Degree Grantor / Ustanova koja je dodijelila akademski / stručni stupanj: **University of Rijeka / Sveučilište u Rijeci**

Permanent link / Trajna poveznica: <https://um.nsk.hr/um:nbn:hr:193:454897>

Rights / Prava: [Attribution-NonCommercial-NoDerivatives 4.0 International/Imenovanje-Nekomercijalno-Bez prerada 4.0 međunarodna](#)

Download date / Datum preuzimanja: **2024-05-23**

Repository / Repozitorij:



[Repository of the University of Rijeka, Faculty of Biotechnology and Drug Development - BIOTECHRI Repository](#)





UNIVERSITY OF RIJEKA  
DEPARTMENT OF BIOTECHNOLOGY  
Graduate program  
Drug research and development

Iva Pavičić

**AAV vector based neonatal desensitization for  
the assessment of cell-replacement therapy  
for Parkinson's disease**

Master's thesis

Lund, 2021.



UNIVERSITY OF RIJEKA  
DEPARTMENT OF BIOTECHNOLOGY  
Graduate program  
Drug research and development

Iva Pavičić

AAV vector based neonatal desensitization for  
the assessment of cell-replacement therapy  
for Parkinson's disease

Master's thesis

Mentor: Andreas Heuer, Assistant Professor

Co-mentor: Jelena Ban, Assistant Professor

Lund, 2021.



SVEUČILIŠTE U RIJECI  
ODJEL ZA BIOTEHNOLOGIJU  
Diplomski sveučilišni studij  
Istraživanje i razvoj lijekova

Iva Pavičić

Neonatalna desenzibilizacija u istraživanju  
transplantacijske terapije za Parkinsonovu  
bolest bazirana na AAV vektorima

Diplomski rad

Mentor: doc. dr. sc. Andreas Heuer

Komentor: doc. dr. sc. Jelena Ban

Lund, 2021.



## **Acknowledgment**

I would like to thank Asst. Prof. Andreas Heuer for giving me the opportunity to conduct my master thesis research as a part of the Behavioural Neuroscience Laboratory (BNL) at Biomedical Centre of Lund University, Sweden. I am extremely grateful for his endless support and encouragement. Special thanks to Matilde Negrini, for her very valuable guidance and kindness during my internship. I would also like to thank Francesco Gubinelli, PhD, and all members of the BNL for their endless support. Also, I would like to thank Asst. Prof. Jelena Ban for the encouragement and help during my internship. Lastly, I want to thank my friends and family who were always encouraging and supporting me during my faculty.



Master's thesis was defended on September 14, 2021

in front of the committee:

1. Andreas Heuer, Assistant Professor
2. Jelena Ban, Assistant Professor
3. Rozi Andretić Waldowski, Associate Professor.
4. Igor Jurak, Associate Professor

This thesis has 42 pages, 7 figures, 42 references



## Abstract

With over ten million diagnoses worldwide, Parkinson's disease (PD) is the second most common neurodegenerative disease. The disease is characterized by progressive loss of dopaminergic neurons in *substantia nigra pars compacta* (SNpc), expressed through the various motor and non-motor symptoms. One of the most promising therapies for PD is cell – replacement therapy. The first clinical trials for cell-replacement therapy were in the 1980s and they involved the transplantation of foetal tissue rich in dopaminergic neurons to patients with an advanced type of the disease. Nowadays, Human Embryonic Stem Cells (hESCs) are used in transplantation therapy for PD and several other degenerative diseases. Nevertheless, this approach has a major drawback. The preclinical safety assessment of hESCs comprises of the *in vivo* experiments on animals, which includes transplantation of xenografts and strong activation of the host's immune system. To surpass this problem immune-incompetent or immune-suppressed animals are used. Though the suppression of the host's immune system is a viable approach, it is not sustainable for the long-term assessment of treatment with hESCs. Neonatal desensitization is the third method that can be used in the evaluation of hESC for cell-replacement therapy in PD. The principle of neonatal desensitization is based on the presentation of the human antigens (by injection of cell suspension) to the host's immune system in the early stages of its development (e.g., up to 5 days after birth in rats). After the desensitization, the host's immune system is "tricked" and the engrafting with the same cell type results in the integration and acceptance of the xenotransplant. However, the problem of this approach is that the differentiation of the cells used for desensitisation must be timely matched to the birth of the recipients. Therefore, we propose a new approach for desensitization based on the overexpression of surface antigens present on



the H9 hESC line via adeno-associated virus (AAV) vectors. We have successfully identified the surface antigens present on the H9 hESC line. Also, we have confirmed that by using cytomegalovirus (CMV)  $\beta$  actin (CBA) promoter we can accomplish viral expression in 5 days. Finally, we have successfully created a library of AAV vectors expressing HLA class I molecules found on the H9 hESC line.

**Key words:**

Parkinson's disease (PD), cell-replacement therapy, neonatal desensitization, AAV vector, H9 hESC line, HLA class I molecules



## Sažetak

Parkinsonova bolest (PD) je druga najčešća neurodegenerativna bolest, koja zahvaća više od 10 milijuna pacijenata diljem svijeta. Glavna karakteristika bolesti je progresivan gubitak dopaminergičkih neurona u *substantia nigra pars compacta* (SNpc) regiji, koji se očituje kroz specifične motoričke i nemotoričke simptome. Jedna od terapija za PD je I transplatacijska terapija kojom se nadomješta gubitak dopaminergičkih neurona. Prva klinička ispitivanja za transplantacijsku terapiju uključivala su transplantaciju fetalnog tkiva, bogatog dopaminergičkim neuronima, kod pacijenta s uznapredovalim stadijom bolesti. Danas se u transplantacijskoj terapiji za PD koriste embrionalne matične stanice (eng. hESC). Ipak, korištenje matičnih stanica u transplantacijskoj terapiji ima i svoje nedostatke. Pretklinička istraživanja o sigurnosti transplantacijske terapije s matičnim stanicama sastoje se od *in vivo* pokusa na životinjama, što uključuje transplantaciju ksenografta i snažnu aktivaciju imunološkog sustava domaćina. Kao rješenje ovog problema, u trenutnim istraživanjima koriste se imunodificijentne ili framakološki imunološki potisnute životinje. Iako je supresija imunološkog sustava domaćina održiv pristup u kratkoročnom periodu, dugoročna analiza nije moguća. Kao treće rješenje predstavlja se desenzibilizacija mladunaca životinja, koja se pokazala kao valjana metoda dugoročne analize u transplantacijskoj terapiji. Načelo neonatalne desenzibilizacije temelji se na prezentaciji ljudskih antigena (injekcijom stanične suspenzije) imunološkom sustavu domaćina u ranim fazama njegova razvoja (npr. do 5 dana nakon rođenja kod štakora). Nakon desenzibilizacije imunološki sustav domaćina je prilagođen, te transplantacija istog tipa stanica rezultira integracijom i prihvaćanjem ksenotransplantata. Međutim, problem ovog pristupa je što se diferencijacija stanica korištenih za desenzibilizaciju, mora pravodobno uskladiti s rođenjem primatelja. Stoga predlažemo novi pristup



desenzibilizaciji, koji se temelji na prekomjernoj ekspresiji površinskih antigena prisutnih na liniji H9 embrijonalnoj matičnoj liniji koristeći adeno-povezane virusne (AAV) vektore. U našem istraživanju uspješno smo identificirali površinske antigene prisutne na H9 staničnoj liniji. Također smo potvrdili da upotrebom promotora citomegalovirusa (CMV)  $\beta$ aktina (CBA) možemo postići virusnu ekspresiju u 5 dana. Konačno, uspješno smo stvorili biblioteku AAV vektora koji izražavaju molekule HLA I razreda, prisutne na H9 staničnoj liniji.

**Ključne riječi:**

Parkinsonova bolest (PD), transplantacijska terapija, neonatalna desenzibilizacija, AAV vektor, H9 stanična linija, molekule HLA I razreda



## Contents

<i>1. Introduction</i> .....	<i>1</i>
1.1. Clinical characteristics of Parkinson's disease .....	1
1.2. Pathology of PD.....	1
1.3. Heritability of PD .....	3
1.4. Environment and PD .....	4
1.5. Treatments for PD .....	5
1.5.1.Cell replacement therapy in PD.....	6
1.6. Neonatal desensitization.....	6
1.7. human Embryonic Stem Cells (hESC).....	10
1.8. Human Leukocyte Antigen (HLA) system .....	10
1.8.1.HLA class I molecules.....	11
1.8.2.H9 hESC line and HLA class I .....	12
<i>2. Aim of the study</i> .....	<i>13</i>
<i>3. Materials and Methods</i> .....	<i>15</i>
3.1. Research animals .....	15
3.2. Injections .....	15
3.3. Tissue preparation .....	16
3.4. Immunohistochemistry.....	17
3.5. RNA extraction and PCR .....	18
3.6. Imaging .....	20
3.7. Molecular Cloning .....	20
<i>4. Results</i> .....	<i>22</i>
4.1. Transplantation of H9-hESC in immune-competent rats results in strong neuroinflammation .....	22



4.2. Injection of CMV-GFP and CBA-GFP AAV vectors did not provide information about time-dependent expression .....	24
4.3. Injection of CBA-aSyn AAV vector provided sufficient information about time-dependent expression .....	27
4.4. Construction and validation of the CBA-HLA class I AAV vectors	29
5. <i>Discussion</i> .....	34
6. <i>Conclusion</i> .....	38
7. <i>Literature</i> .....	39



# 1. Introduction

## 1.1. Clinical characteristics of Parkinson's disease

Parkinson's disease (PD) is the second most common degenerative disease of the central nervous system (CNS), affecting 1–2 people per 1000 of the population (1). The disease was first described in 1817 by English scientist James Parkinson, who described it as: *"shaking palsy, disease accompanied by involuntary tremulous motion, with lessened muscular power"* (2). At the onset, PD affects people at the mean age of 55 years (3) and the incidence increases to 11–12 people per 1000 of the population at the age of 70 (1).

PD is characterized as a progressive movement disorder that manifests through four cardinal motor symptoms represented under the acronym TRAP. TRAP includes the following symptoms: Tremor at rest, Rigidity, Akinesia (or bradykinesia), and Postural instability (4). Although TRAP symptoms are the most prominent motor symptoms of the disease, PD can be displayed through other symptoms such as impaired gait and precision grip deficits (5). Besides the motor symptoms, PD can also manifest through other non-motor symptoms such as cognitive impairment, depression, apathy, dysautonomia (e.g., constipation, orthostatic hypotension, rapid eye movement behaviour disorder) and others (4).

## 1.2. Pathology of PD

With over ten million diagnoses worldwide, PD is a rising threat for societies with long life expectancy. Today approximately 90% of all PD cases are referred to as sporadic type with no direct genetic linkage, whereas the rest of the cases are referred to as a familial type of PD (6). Besides sporadic



and familial types of PD, the disease can manifest following intoxication, infection, head trauma etc. (7). Although the cause of PD remains elusive, all diagnoses have one thing in common: loss of nigrostriatal dopaminergic neurons in the *substantia nigra pars compacta* (SNpc) (8).

Dopamine (DA), a monoamine neurotransmitter, is produced by dopaminergic neurons found in various regions of the brain. Dopaminergic neurons are especially abundant in the *substantia nigra* (9). Cell bodies of nigrostriatal dopaminergic neurons are found in SNpc, but they project into the striatum of the brain. The characteristic trait of dopaminergic neurons found in the SNpc, is the presence of the pigment melanin in their cell bodies. Therefore, with the advancing of the PD the loss of neuromelanin in patients can be observed. Reduction of pigmentation is proportional with the loss of expression of the DA transporter (DAT) mRNA and with the decrease of DA in the striatum, the main projection area of dopaminergic neurons (3).

Formation and spread of the intraneuronal inclusions like Lewy body (LB) and Lewy neurites in the substantia nigra is another neuropathological hallmark of the late PD (10). The LB structures are formed as a result of misfolding and aggregation of  $\alpha$ -synuclein (aSyn) protein (7).  $\alpha$ -synuclein is a neuronal protein, part of the synuclein family of proteins, that are highly abundant in the brain. The synuclein family is made up of three proteins:  $\alpha$ -synuclein,  $\beta$ -synuclein and  $\gamma$ -synuclein. Although numerous studies about  $\alpha$ -synuclein protein have been published, the exact role of the protein remains elusive. Studies have shown that both  $\alpha$ -synuclein and  $\beta$ -synuclein function could be correlated with vesicular transport in the cell (10). In the study published by Jenco et al. (11) it was shown that both  $\alpha$ -synuclein and  $\beta$ -synuclein can selectively inhibit phospholipase D2, an isoform of phospholipase D, involved in signal-induced cytoskeletal regulation and



endocytosis (11). Besides PD, the toxicity of  $\alpha$ -synuclein has been linked to two other disorders, Multiple System Atrophy (MSA) and Dementia with Lewy Bodies (DLB) (12).

### 1.3. Heritability of PD

The first described cause of familial PD was a point mutation of amino acid alanine – threonine at position 53 (A53T) at N-terminal domain of the  $\alpha$ -synuclein protein, identified in Greek kindreds with early onset of PD (13). Moreover, the point mutation alanine–proline at position 30 (A30P), point mutation glutamic acid–lysine at position 46 (E46K) and point mutation histidine–glutamine at position 50 (H50Q), all correlated with the monogenetic familial type of PD. Interestingly, all point mutations are located in the N-terminal domain of the protein (12). These point missense mutations lead to the formation of a stable secondary structure of  $\alpha$ -synuclein, which is natively unfolded. Change in the secondary structure of the protein results in the advanced formation of toxic oligomers, protofibrils and fibrils (14). Apart from the point mutations in the gene encoding for  $\alpha$ -synuclein protein, missense and nonsense mutations in the Leucine–Rich Repeat Kinase 2 (LRRK2) gene have been associated with late-onset PD (14). The mutation glycine–serine at position 2019 (G2019S) is the most frequent mutation in the LRRK2 gene associated with PD that accounts for 5–6% of familial cases of PD (15). Both the mutations in  $\alpha$ -synuclein and LRRK2 gene are correlated with the onset of autosomal–dominant PD. Also, mutations in the LRRK2 can be linked to both familial and sporadic types of PD.

*Parkin* (PARK2) was the first gene linked with the early onset autosomal – recessive PD. Multiple mutations of PARK2, including point mutations, deletions and duplications, have been linked to the cause of early–onset PD



(EOPD) (14). Mutations in the PARK2 gene are associated with over 10% of total EOPD cases (14), making them the most common cause of EOPD to this day. Other genes linked with autosomal-recessive PD are: phosphate and tensin homolog (PTEN)-induced putative kinase 1 (PINK1) and DJ-1 (PARK7) (16). The PINK1 gene is the second most common cause of AR EOPD (14). Various nonsense and missense mutations in the PINK1 gene have been linked to the onset of the disease. On the other hand, mutations in the DJ-1 gene are a very rare cause of the PD, affecting only 1 – 2% of cases (14).

However, the aforementioned genes are not the only genes linked to the manifestation of PD. Over the years Genome-Wide Association Studies (GWAS) have revealed that several genes can be considered as risk factors for developing PD. Some of them include Microtubule Associated Protein Tau (MAPT), Apolipoprotein E (APOE),  $\beta$  - glucocerebrosidase (GBA) and others (14). Interestingly, the GBA gene, encoding for  $\beta$  - glucocerebrosidase protein involved in lysosomal metabolism of glycolipids, has been associated with a monogenic type of PD (16) as well, but the exact mechanism remains unclear.

#### 1.4. Environment and PD

With only approximately 10% of patients diagnosed with familial, genetically linked PD, the cause of PD for the remaining percentage of patients, remains unknown. A big effect on the onset of the disease could be gene-environment interaction. Some of the environmental contributors that have been linked to the onset of PD include exposure to chemicals (e.g., pesticides, herbicides) and solvents (e.g., trichloroethylene), heavy metals (e.g., iron and copper) etc. (6,17). For example, the protoxin 1-methyl-4-phenyl-1,2,3,6-tetrahydropyridine (MPTP), a by-product in the



synthesis of heroin, induces PD by selective inhibition of dopaminergic neurons (18). Exposure to environmental toxins like pesticides (e.g., rotenone) and herbicides (e.g., paraquat) has been shown to induce neuropathological features of PD (19). More recently there have been studies showing the correlation of the exposure to the industrial solvent trichloroethylene (TCE) and induced activity of LRRK2 kinase in the rat model of PD (17). In addition to exposure to potential environmental risk factors, different socioeconomic circumstances could also affect the onset of the disease.

### 1.5. Treatments for PD

The gold standard for the treatment of PD is therapy with levodopa (3,4-dihydroxy-l-phenylalanine) (L-DOPA), a precursor molecule in the synthesis pathway of DA. Currently, therapy with L-DOPA is combined with the administration of inhibitors of dopa decarboxylase (DDC) and catechol-O-methyltransferase (COMT) (20). Although treatment with L-DOPA is still considered a gold standard, it is far from ideal. When administered over a longer period, L-DOPA can cause adverse effects such as dyskinesias (uncontrolled, involuntary movements) and development of motor fluctuations (21).

Another mode of therapy used for the treatment of PD is Deep Brain Stimulation (DBS). It is based on the high-frequency stimulation of the subthalamic nucleus using implanted microelectrodes (22). However, DBS is invasive, and requires optimization of the stimulating parameters to each patient, which is a big disadvantage.



### 1.5.1. Cell replacement therapy in PD

The focus of cell-replacement therapy in PD is to make up for the loss of dopaminergic neurons in the SNpc which get degenerated as the disease progresses. The principle of the approach is to transplant the dopaminergic neurons which restore DA transmission in the nigrostriatal pathway and thus result in the relief of the symptoms and improvement of quality of living. In 1987 first trial for cell replacement therapy in PD started where patients were transplanted with intrastriatal tissue of foetal mesencephalic tissue rich in dopaminergic neurons (23). Two of the patients that have been involved in the initial trial showed long-term survival of the transplant (24), but overall, the study did not reach success. Although it was reported that two subjects who have had long-term survival of the transplant, developed  $\alpha$ -synuclein positive Lewy bodies (24), the progression of the disease pathology was very slow. Moreover, the survival period of the transplants in the different patients was dependent on the regimen of immunosuppressive therapy they received. Another big problem in cell replacement therapy in PD is immune compatibility between donor and host, as the transplant induces activation of the host immune system, accompanied by activation of macrophages and microglia at the transplant site (25). All in all, cell-replacement therapy is a promising choice in the treatment of PD, especially in younger patients with a mild type of the disease.

### 1.6. Neonatal desensitization

Although cell-replacement therapy for the treatment of PD has been present since the 1980s, certain segments need improvement. A big part in the safety assessment of any therapy or drug is the preclinical phase. The preclinical phase consists of *in vitro* and *in vivo* experiments. A major



drawback in the assessment of cell-replacement therapy for the treatment of PD is the *in vivo* experiments. In this case, *in vivo* experiments imply transplantation of cells (other than human for ethical reasons), resulting thus in the activation of the host's immune system and rejection of the xenotransplant. Consequently, there is no ability to do a behavioural assessment after the transplantation of xenografts. Currently, to overcome this problem, *in vivo* studies on rats, depend on using either immune-incompetent or immune-suppressed animals. The first approach is based on using nude-athymic rats, immune-incompetent host animals, lacking thyroid gland. However, the major disadvantage of using nude rats is at the same time its biggest advantage. Using an immune-incompetent host animals (e.g., nude athymic rats), that do not have a developed immune system, makes them especially prone to infections, and working conditions extremely difficult and expensive. The other option is using wild type rats whose immune system can be suppressed pharmacologically. Commonly, the immunosuppressive drug cyclosporine is used in this approach. However, the biggest drawback of using cyclosporine is its nephrotoxicity after 20 weeks of daily administration. As human cells do require considerable amounts of time for maturation, this limits the preclinical assessment of fully mature grafted cells. Given all the possibilities there is no optimal model that can be used for behavioural assessment after transplantation of xenografts.

With the rise of preclinical trials for cell replacement therapy in the treatment of PD, the scientific focus has been on validation of survival and safety of the chosen transplanted cells in animal models. As mentioned before, immunosuppressive drugs or immune-incompetent animal hosts have been a gold standard in the research of transplantation of neuronal xenografts in PD.



In the 1950s, a paper by R.E. Billingham, L. Brent and P.B. Medawar was published, in which they described for the first time the acquired tolerance of foreign cells in new-born animals (26). In the paper, they described the phenomenon as actively acquired tolerance (26). In the experiment, they used two different strains of mice: strain A and strain CBA. Firstly, a foetal mouse of one strain (e.g., strain CBA) is inoculated *in utero* with a suspension of cells from the mouse of another strain (e.g., strain A). After maturation, adult CBA mice would be partially or fully tolerant of grafts transplanted from the mouse of the strain of original donor (26). Moreover, they have shown that grafts transplanted from the mouse belonging to the strain of original donor outlived grafts transplanted from the third strain (e.g., strain AU) (27). Nowadays, the term neonatal desensitization has become a synonym for the phenomenon known as actively acquired tolerance.

Since the original paper about neonatal desensitization has been published, different groups have focused on trying to achieve the same. The exact mechanism underlying this phenomenon remains unknown. One of the most important factors in achieving neonatal desensitization is a short time window in which the immune system of the host animal can be desensitized. Billingham et al. have shown that the transplantation of xenografts to adult animals caused a very strong immune response, contrary to transplantation of xenografts in utero (27). More recently, a paper was published whereby achieving neonatal desensitization neuronal xenotransplants had long – term survival rate (28). Kelly et al. desensitized rat neonates (up to 10 days of age) by injection of cell suspension of either human or mouse donor tissue at the day of the birth (28). After the maturation of the pups, they were challenged with transplantation of the cells, where both human and mouse desensitized rats did not show evidence of ongoing rejection (28). In addition, rats were desensitized at



different time points after which they received a xenotransplant. Only rats desensitized up to 5 days after birth showed good transplant survival, thus implying the importance of desensitization during an early neonatal stage.

Contrary to the article published by Kelly et al., in a study published by Walczak et al. (29) neonatal desensitization did not prevent xenograft rejection. The experiments were conducted on both mice and rats, and in both cases, neonatal desensitization did not prevent rejection of transplanted human cells (29). However, there are a few probable explanations for the unsuccessful desensitization and poor graft survival. Firstly, the experiments were done on Wistar rats, not on Sprague – Dawley (SD) rats used in the paper by Kelly et al. (28). Also, the cells used for the desensitization in that study were non transformed neuronal stem cells derived from the human umbilical cord (HUBC-NSC) (29), which differ from the cells used in the experiments where desensitization was successful. Lastly, the authors did not specify the age of the animals at the time of the inoculation, which can be a critical point in achieving desensitization.

Besides the paper by Kelly et al. (28), an article was published recently by Heuer et al. (30) in which neonatal desensitization has prevented the rejection of xenografts. In the study, rats have been desensitized with cell suspension containing both differentiated and undifferentiated cells from two different hESC lines: H9 and RC17. After maturation adult animals have been transplanted with differentiated H9, RC17 or induced neuronal (iN) cells derived via direct neural conversion of human foetal lung fibroblasts on the post-natal day 2 (30). Adult animals engrafted with either hESC did not reject transplant and the survival rate of the xenotransplant was similar to the survival rate of xenotransplant in immune-suppressed group (30). On the other hand, animals transplanted with iN cells evoked strong immune response and rejection of xenotransplant. Results of this study



emphasized the principles of achieving neonatal desensitization: neonatal age of the animals and the choice of the cell line used for desensitization.

### 1.7. human Embryonic Stem Cells (hESC)

The first isolation of Human Embryonic Stem Cells (hESC) happened in 1998., when Thomson et al. (31) reported the isolation of human – blastocyte derived pluripotent cells: hESC. hESC are derived from the inner cell mass (ICM) of the human embryo and are pluripotent cells, with an ability to differentiate in any cell lineage. In the work published by Thomson et al. (31), hESC had normal karyotypes and they expressed high telomerase activity as well as specific cell surface markers characteristic for hESC. They described five cell lines derived from five different embryos: H1, H13 and H14 with XY karyotype and H7 and H9 with XX karyotype (31). Interestingly, the H9 line successfully had been cultured for more than eight months surpassing other cell lines that have been isolated. Today, even with the number of the reported hESC lines increasing rapidly, the H9 line, with its derivatives, remains one of the most widely used cell lines in stem cell research (32).

### 1.8. Human Leukocyte Antigen (HLA) system

In homeostasis conditions, all protein molecules undergo the process of degradation and new synthesis. Degradation of most proteins can be done in two pathways: lysosomal and ubiquitin–proteasome pathway (33). The lysosomal pathway includes proteins taken up from the extracellular matrix by endocytosis or proteins for cytosol taken up by autophagy. On the other hand, the ubiquitin–proteasome pathway degrades cytosolic proteins (e.g., regulatory protein, misfolded or defected proteins) (33). To scan for any possible signs of unbalanced homeostasis, oligopeptides from degraded



proteins are presented to cells of the immune system (i.e., T cells) by major histocompatibility complex (MHC). The human leukocyte antigen (HLA) system is the human variant of MHC. The HLA complex is encoded by more than 40 genes, located on the p arm on chromosome 6 (34), with over 30 000 alleles, making it extremely polymorphic. The HLA system can be divided into two classes: HLA class I and HLA class II, which differ both structurally and functionally. Firstly, HLA class I molecules are presented on the surface of most cell types, whereas HLA class II molecules are presented on certain cells of the immune system. Moreover, the oligopeptides from ubiquitin–proteasome pathway are presented on HLA class I molecules, whereas lysosomal oligopeptides are presented on HLA class II molecules.

#### 1.8.1.HLA class I molecules

Since HLA class I molecules are present on most cell types in humans, their function can be described as general. The structure of HLA class I molecules consist of two polypeptides that are non-covalently bound. The  $\beta$ 2-microglobulin ( $\beta$ 2m) is the light chain of the class I molecule, whereas the  $\alpha$  chain is the heavy chain of the molecule. The  $\alpha$  chain is divided into three major domains:  $\alpha$ 1 and  $\alpha$ 2 which are peptide-binding domains and  $\alpha$ 3 which is an immunoglobulin–like domain. In addition, class I molecules have a transmembrane region (TM) and cytoplasmic tail (CYT) (35).

There are three different HLA class I molecules: HLA-A, HLA-B and HLA-C. To this day more than 20 000 alleles for HLA class I have been reported. The highest degree of polymorphism has been detected in the peptide–binding region of the molecule, making a unique library of specific variants for the binding of peptide ligands (36). Even though HLA class I molecules come in many different variants, they can be gathered into groups, termed



supertypes. Each supertype is constituted of molecules that share largely overlapping peptide binding specificity (36).

### 1.8.2. H9 hESC line and HLA class I

As mentioned above, H9 hESCs are pluripotent cells that can differentiate into any cell type. The ability of hESC to differentiate into any cell type has made them a very valuable tool in the treatment of various degenerative diseases (e.g., PD, spinal cord injury (SCI) etc.). However, transplantation of hESC as a potential treatment for a specific disease, does not work in such a straightforward way. To overcome the immunogenic properties of hESC and rejection of the graft, matching of MHC alleles should be performed before the transplantation. It has been shown that there is a difference in expression of MHC class I and MHC class II molecules in undifferentiated and differentiated hESC (37). Undifferentiated hESC express low levels of MHC class I molecules, while MHC class II molecules are not expressed at all (37). The H9 hESC line has been classified based on the HLA alleles. It has been shown that the H9 cell line has the following set of HLA class I alleles: HLA-A (A\*02:01:01, A\*03:01:01), HLA-B (B\*35:03, B\*44:02:01) and HLA-C (C\*04:01:01, C\*07:04) (38).



## 2. Aim of the study

Transplantation of hESC has risen as a possible solution for the treatment of PD. To use hESC as an established therapy in PD and to assess therapeutic effects on motor symptoms, *in vivo* behavioural experiments on animals must be carried out prior. However, this assessment has a big limitation. It includes transplantation of xenografts, which without immunosuppressive drugs results in a complete rejection.

Neonatal desensitization is a novel approach, which has been shown as a feasible solution to this problem. Neonatal desensitization is a method in which the host's immune system is "tricked" into recognizing foreign (i.e., human) tissue as self, by exposing the adaptive immune system of newborn animals to human antigens. Currently, neonatal desensitization is achieved by intraperitoneal (i.p.) injection of differentiated hESC suspension. It is dependent on the right timing of the birth of animals and differentiation of hESC to the right timepoint. The problem with this approach is that the differentiation of the cells used for desensitisation must be timely matched to the birth of the recipients. An off the shelf approach would overcome this limitation.

Therefore, we aim to develop a new way to achieve neonatal desensitization by using adeno-associated virus (AAV) vectors overexpressing MHC-I and MHC-II proteins found on the surface of the H9 hESC line via intramuscular (i.m.) injection at the time of birth. To achieve the mentioned approach, we set the following goals in this thesis:

1. Analysis of surface markers expressed on the surface of H9 hESC line
2. Optimization and validation of expression of cytomegalovirus (CMV) and cytomegalovirus chicken  $\beta$ -actin (CBA) promoters by i.m. injection of AAV vectors



### 3. Creating a library of plasmid vectors carrying a gene for specific surface markers of the H9 hESC line

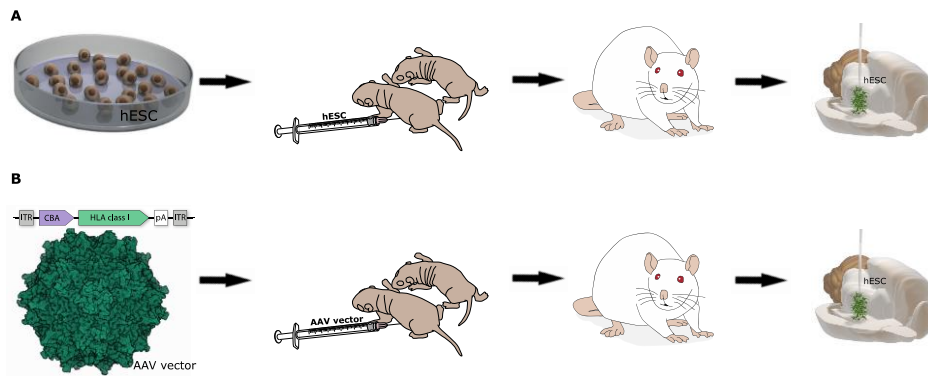


**Figure 1 Schematic flow diagram comparing current and proposed method for achieving neonatal desensitization.** Schematic illustration of the process order in the current way of doing neonatal desensitization (A) and the new method proposed in this study (B). In brief, currently neonatal desensitization is achieved by injection of hESC into new-born animals. After maturation, animals are transplanted with hESC derived grafts. In our approach animals would be desensitized using an AAV vector that contains genes encoding for HLA class I molecules found on the surface of hESC.



## 3. Materials and Methods

### 3.1. Research animals

All experiments conducted in the present study were carried following relevant guidelines and regulations. All experimental protocols were approved by the local ethical committee at Lund University. Female adult tyrosine hydroxylase Cre recombinase (TH:Cre<sup>+/-</sup>)-SD rats were used for this study.

### 3.2. Injections

Before all surgical procedures, rats have been anaesthetised using a gaseous isoflurane/O<sub>2</sub> mixture. Intramuscular injections were performed using a 10 µl Hamilton syringe. Injections were carried out in two rounds. For the first round we used the CMV-GFP AAV vector and CBA-GFP AAV vectors, injected bilaterally into the *vastus intermedius* muscle of the same animal. In the second round, the CBA-aSyn AAV vector was injected unilaterally into the *gastrocnemius* muscle. The AAV vectors (Figure 2.) were matched to a titter of  $1 \times 10^{12}$  gc/ml. A total volume of 2 µl for each round was injected with an additional three minutes allowing the diffusion, before carefully removing the syringe.

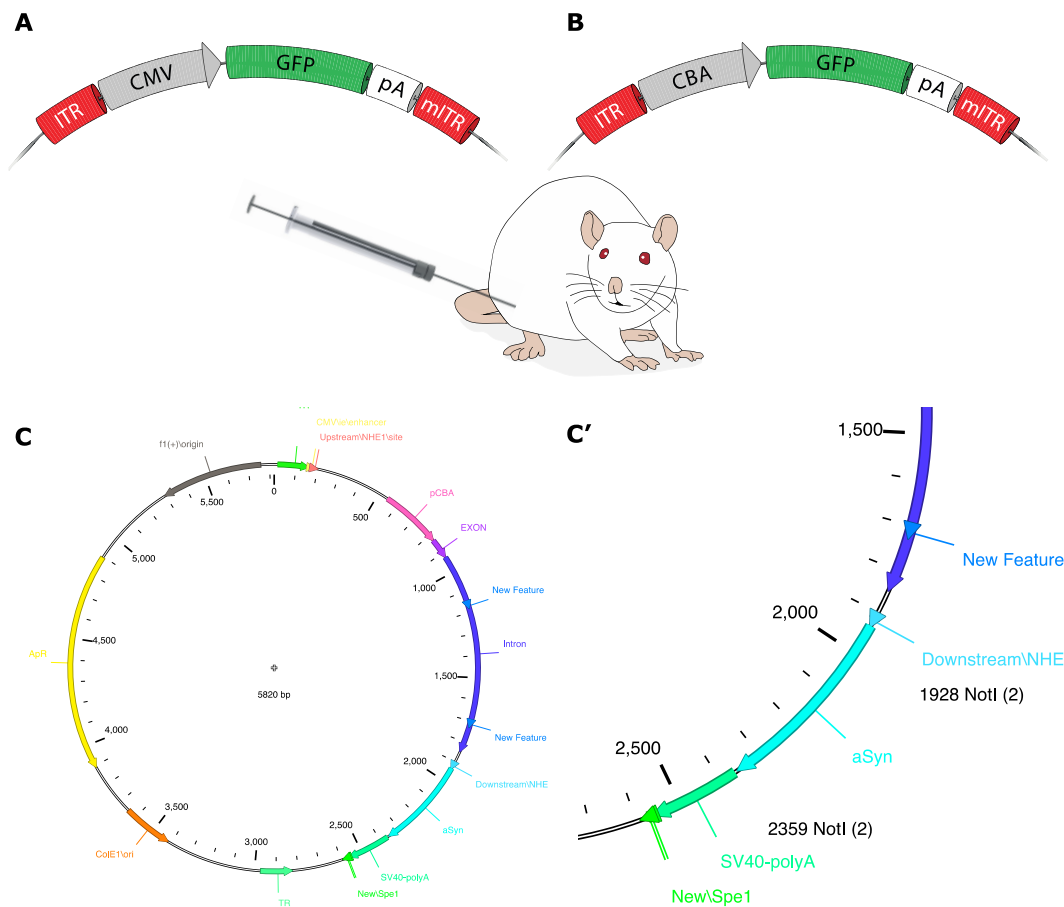


**Figure 2 Illustrations of three different plasmids constructs used in this study.** Schematic representation of two plasmids containing gene encoding for GFP used for the validation part of this study: CMV promoter-based plasmid (A) and CBA promoter-based plasmid (B). Plasmid map of the CBA-aSyn plasmid used in validation and cloning part of this study (C), with the close-up image showing NotI restriction sites used for the digestion of the plasmid backbone (C').

### 3.3. Tissue preparation

Five and four days, respectively, after AAV-injections rats have been sacrificed with pentobarbital overdose and perfused via injections of saline through the heart, followed by ice-cold 4% paraformaldehyde (PFA) solution. The muscles were stored in 4% PFA solution for 24h and transferred to 30% sucrose solution until sunk. The fixed tissues were subjected to graded ethanol and isopropanol series (both Fisher Scientific,



UK) before paraffin embedding (Histolab, Sweden). 5  $\mu$ m thick sections were cut on a microtome (Leica) and placed on gelatin covered microscope slides (VWR, Sweden).

### 3.4. Immunohistochemistry

Immunohistochemical stainings were performed as described elsewhere (30). For paraffin-embedded tissue, gradual rehydration and deparaffinization was performed before immunohistochemical staining. The rehydration process was graded as follows: xylene (3min, 2x), 99.5% ethanol (3min, 2x), 95% ethanol (3min), 70% ethanol (3min) and deionized water (3min). Immunohistochemical stainings were performed on the gelatin covered microscope slides. To preserve sections from drying out, the borders of each slide were lined with ImmEdge™ Pen (H-4000) (Vector Laboratories, Sweden) and left to dry. A list of primary and secondary antibodies used in this study can be found in Table 1. To sum up, sections were washed three times in KPBS (NaCl 137 mmol/L, KCl 2.7 mmol/L, Na<sub>2</sub>HPO<sub>4</sub> 10 mmol/L, KH<sub>2</sub>PO<sub>4</sub> 1.8 mmol/L, pH=7.4), and incubated in 5% serum (based on the species the secondary antibody was raised in) in KPBS-T (KBPS +1% Triton X-100, pH=7.4) for 1 hour at room temperature. Afterwards, sections were incubated in primary antibody in 5% serum at room temperature overnight. The following day, sections were washed two times in KPBS and incubated again in 5% serum, for at least 15 min. Subsequently, sections were incubated in fluorophore-conjugated secondary antibody for 1 hour, following three-step washes in KPBS. Some sections were stained with 1:1000 DAPI (Invitrogen, Thermo Fisher Scientific) in KPBS for 30 minutes, with three additional KPBS wash steps. Sections were cover slipped after 10–15 min using PVA-DABCO.



Table 1 Antibodies used for immunohistochemical analysis in this study

<b>1° Ab</b>	<b>Species</b>	<b>Dilution</b>	<b>Supplier</b>	<b>Serum</b>	<b>2° Ab</b>	<b>Dilution</b>	<b>Supplier</b>
GFP	Chicken	1:10 000	Abcam	Goat	anti- chicken	1:200	Alexa 488, Invitrogen
aSyn	Mouse	1:1000	Santa Cruz Biotechnology	Goat	anti- mouse	1:200	Alexa 568, Invitrogen

### 3.5. RNA extraction and PCR

RNA extraction from muscle samples was performed using E.Z.N.A. FFPE RNA Kit (Omega Bio-Tek, Sweden), following the manufacturer's instructions. In brief, four 5 µm thick paraffin-embedded sections were placed into a 1.5 ml Eppendorf tube containing lysis buffer. The concentration of the RNA was measured using Nanodrop 2000c (Thermo Fisher Scientific). Approximately 100 – 300 ng of total RNA was retrotranscribed into cDNA using iScript cDNA Synthesis Kit (Bio-Rad Laboratories, Sweden). To amplify GFP and human SNCA genes Phusion Hot Start II High-Fidelity DNA polymerase 3-step (Thermo Fisher Scientific, Sweden) assay was used. Initial denaturation cycle at 98°C for the 30s, followed by 25 – 35 amplification cycles in 3 steps: denaturation at 98°C for 10s, annealing for 30 s, and extension at 72°C for 15s. The final extension cycle was at 72°C for 15min. Annealing temperatures were calculated using Tm Calculator ([www.thermofisher.com](http://www.thermofisher.com)). A list of forward and reverse primers (Eurofins, Sweden) and their corresponding annealing temperatures are in Table 2. All PCR products were analysed by running 1% agarose gel electrophoresis in 1x TAE buffer at 90 – 100 V for ~ 50 min and visualized under UV light (ChemiDoc, Bio-Rad Laboratories).

Table 2 List of PCR primers used in this study

Target gene	Primer name	Forward primer	Reverse primer	Melting temperature (°C)	Size (bp)
GFP	GFP_A	5'-CACATGAAGCAGCACGACTT	5'-TGCTCAGGTAGTGGTTGTCG	65	379
GAPDH	GAPDH	5'-CAACTCCCTCAAGATTGTCAGCAA	5'-GGCATGGACTGTGGTCATGA	65	118
human aSyn	haSyn_A	5'-ATGCTCTAGAATGGATGTATTCATGAAAG GACTTTCAAAGGC	5'-ATGCGTCGACTTAGGCTTCAGGTTTCGTAG TCTTGATAC	63	398
human aSyn	haSyn_J	5'-GGACCAGTTGGGCAAGAATG	5'- CTCATTGTCAGGATCCACAGGC	65	71
HLA-A 03:01	NotI_HLA-A	5'-atggcggccgcATGGCCGTCATGGCG	5'-catgcggccgcTCACACTTTACAAGCTGTGAG	63	1120
HLA-B 07:02	NotI_HLA-B	5'-atggcggccgcATGCTGGTCATGGCGC	5'-catgcggccgcTCAAGCTGTGAGAGACACATC	63	1111
HLA-C 07:01	NotI_HLA-C	5'-atggcggccgcATGCGGGTCATGGCG	5'- catgcggccgcTCAGGCTTTACAAGTGATGAG	63	1123



### 3.6. Imaging

Brightfield images were captured using a Leica DMI8 inverted microscope. Fluorescent images were taken by either the same microscope or using a Leica SP8 laser scanning confocal microscope.

### 3.7. Molecular Cloning

DNA inserts were synthesized (GenScript, USA) according to the sequence found on the NCBI website. A list of the HLA alleles synthesized are presented in Table 2. PCR amplification of the inserts was performed using the manufacturer's standard protocol for Phusion Hot Start II High-Fidelity DNA polymerase (Thermo Fisher Scientific, Sweden), with thermal cycles setup as previously described. Forward and reverse primers (Eurofins, Sweden) for amplification of inserts sequences were designed using A plasmid Editor (ApE) software and Tm Calculator ([www.thermofisher.com](http://www.thermofisher.com)). They were designed to amplify the open reading frame (ORF) of inserts with an overhang sequence containing a restriction site for restriction enzyme NotI (Thermo Fisher Scientific, Sweden) and three additional nucleotide bases. A list of forward and reverse primers used can be found in Table 2. Followed by PCR amplification, samples were separated with DNA electrophoresis on 1% agarose gel (100V, ~ 50 min). Agarose gel was visualized under UV light (ChemiDoc, Bio-Rad Laboratories) followed by band excision. Zymoclean™ Gel DNA Recovery Kit (Zymo Research, Sweden) was used for the recovery of DNA from the agarose gel. The concentration of DNA was measured using Nanodrop 2000c (Thermo Fisher Scientific).

Restriction digestion of the plasmid (pCBA-aSyn) (Figure 1C') and DNA inserts was carried out with NotI restriction enzyme (Thermo Fisher



Scientific, Sweden) according to the provided protocol. To prevent self-ligation of the plasmid vector, dephosphorylation of the vector backbone using 2  $\mu$ l FastAP Thermosensitive Alkaline Phosphatase (Thermo Fisher Scientific, Sweden) was done simultaneously with digestion. The sample was first incubated at 37°C for 20 min, followed by the inactivation of the restriction enzyme at 65°C for 15 min. Validation of the successful digestion with DNA electrophoresis on 1% agarose gel (100V, ~ 50 min) was performed. For the DNA inserts, phosphorylation of the fragments was carried out after restriction digestion with T4 Polynucleotide Kinase (Thermo Fisher Scientific, Sweden). In each 1.5 ml tube (Eppendorf, Sweden) 2  $\mu$ l of 10 mM ATP solution and 1  $\mu$ l of T4 Polynucleotide Kinase was added and incubated at 37°C for 30 min.

Ligation of the digested dephosphorylated backbone and phosphorylated DNA inserts was carried out with T4 DNA Ligase (Thermo Fisher Scientific, Sweden). Firstly, the amount of DNA inserts required for 3:1 ligation of 50 ng of the backbone was calculated using NEBio Ligation Calculator (<https://nebiocalculator.neb.com/#!/ligation>). Samples were incubated at room temperature for 20 min and stored after at 4°C.

After the ligation process, DNA was used to transform Sure 2 Supercompetent Cells (Agilent Technologies). Aliquots of 50  $\mu$ l of the competent bacteria were thawed on ice. 5  $\mu$ l of the ligation product was added to each tube and left on ice for 30 min. For transformation bacteria were treated with heat shock: 42°C, 30 s and then transferred back to ice for additional 2 min. 250  $\mu$ l of 1x LB (Luria-Bertani) medium was added, followed by 1h incubation at 37°C and 220 rpm.

Bacteria were plated with glass beads onto agar plates with Ampicillin (Amp) as a selection marker. Plates were incubated overnight at 37°C. The following day, one colony was selected from each clone. Selected colonies were placed in a round-bottom Falcon tube containing ~ 5 ml of the LB medium with Amp and incubated overnight at 37°C and 220 rpm. DNA was



extracted from the bacteria following the ZymoPURE™ Plasmid Miniprep Kit (Zymo Research, Sweden). Firstly, Falcon tubes with bacteria were centrifuged at 4000 xg for 5 min. Afterwards, the supernatant was discarded while the pellet was resuspended in the provided buffer solution. The samples were then transferred to a 1.5 ml tube (Eppendorf, Sweden) and treated following the manufacturer's protocol. The concentrations of the DNA were measured spectrophotometrically with Nanodrop 2000c (Thermo Fisher Scientific).

To check if the cloning was successful, the samples were digested with both SmaI restriction enzyme (Thermo Fisher Scientific, Sweden) and the combination of two specific restriction enzymes: XbaI (Thermo Fisher Scientific, Sweden) and, KpnI (Thermo Fisher Scientific, Sweden) or PpuMI (Psp5II) (Thermo Fisher Scientific, Sweden). The samples were visualized under the UV light after being separated with DNA electrophoresis on 1% agarose gel (90V, ~ 70 min). In the case of the HLA-A clone, the process after transformation was repeated once more.

## 4. Results

### 4.1. Transplantation of H9-hESC in immune-competent rats results in strong neuroinflammation

In the previous study done by Heuer et al. (30), fully immune-competent rats were transplanted with H9-hESC-derived cells. Assessment of the transplant rejection was measured via activation of the host's immune system over three-time points: 2 weeks, 6 weeks, and 18 weeks. When staining for the marker of microglial activation (Ox42), the strongest inflammation was observed at 6 weeks' time point (Figure 3B). Although microglial cells are the primary innate immune cells of the CNS, strong activation at an early time point was not detected (Figure 3A). Complete minimization of the inflammation was noticed at the 18-week mark (Figure

3C). As mentioned before, H9 hESCs are immunogenic as they express MHC molecules on the surface of the cell. Therefore, the sections were stained for Ox6, a specific marker for MHC class II molecules. Same as it was in the case of Ox42 marker, the strongest expression of MHC class II molecules was at 6 weeks post-transplantation (Figure 3E).

The expression of MHC class II molecules was robust and noticeable even in the 2 weeks' time point (Figure 3D), with the diminishing expression at 18 weeks (Figure 3F).

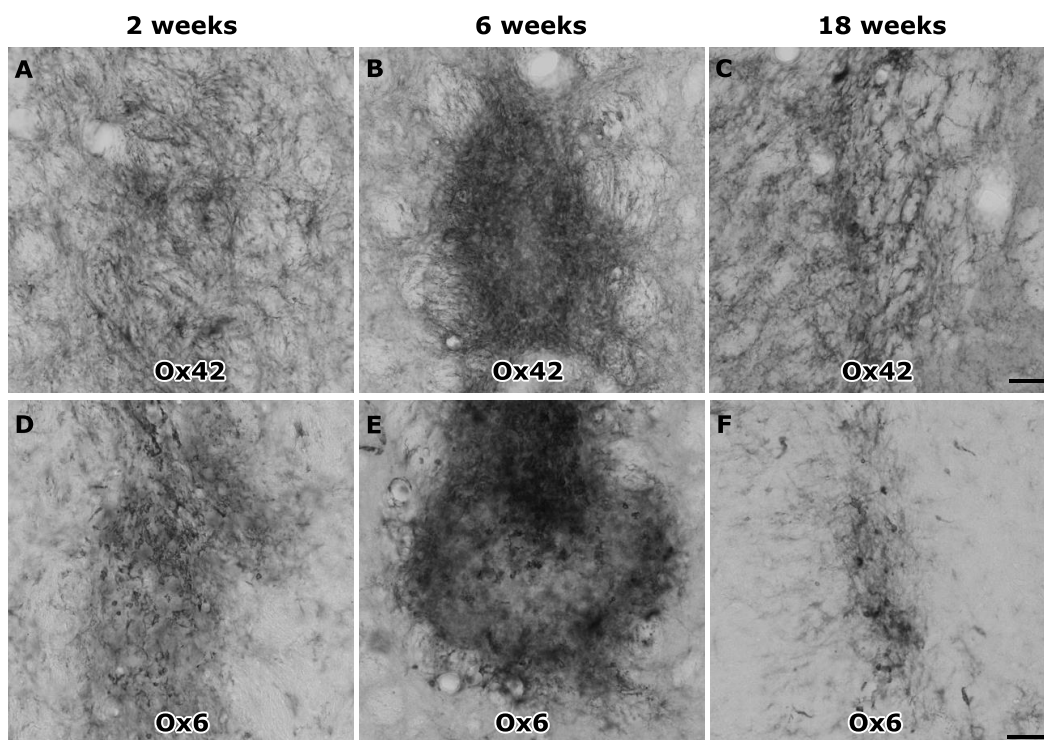


**Figure 3 Transplantation of the engrafted H9 hESC evokes a strong immune response in the immune-competent animals.** Representative images of the immunohistochemical stainings (associated markers on each image) for microglial activation (A-C) and upregulation of MHC class II molecules (D-F) at three different time points. Scale bars represent 50  $\mu$ m.

Furthermore, double staining for the markers CD4 and CD8 was performed. CD4 is a marker for CD4 receptor, found on the T helper cells, while CD8 is a marker for T killer cells. In this instance, the highest intensity of the immune activation was detected at the earliest assessment's time point (Figure 4A). Lastly, the survival of the transplant was assessed after doing the staining for the human neuronal cell adhesion molecule (hNCAM).



hNCAM staining produced stronger intensity in the assessment of 2 weeks old transplant (Figure 4C), when compared to 6 weeks old transplant (Figure 4D), suggesting that the survival rate of the transplant was decreasing upon the activation of T killer cells.

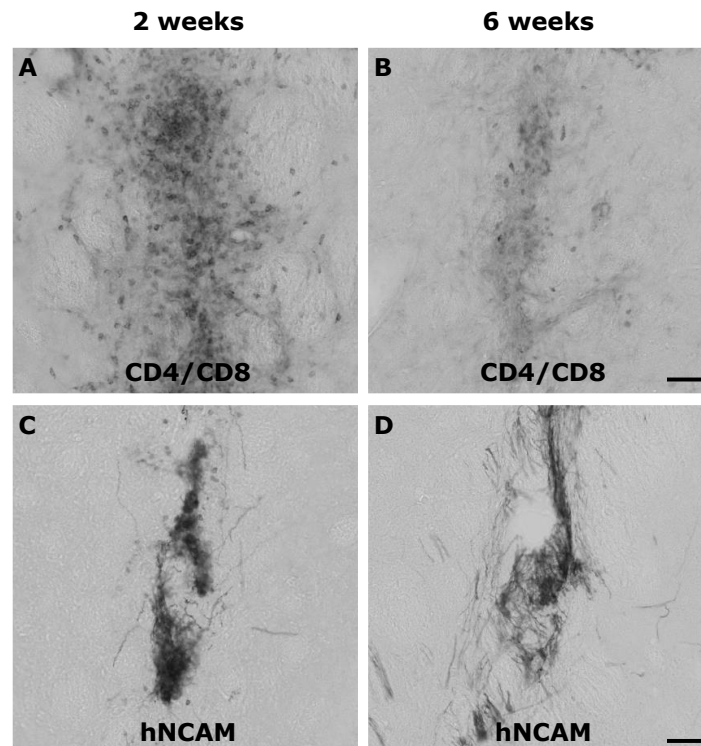


**Figure 4 Activation of the adaptive immune system results in the decrease of the transplant's survival rate.** Representative images of the double immunohistochemical staining against T killer cells (A-B) and hNCAM marker (C-D) at 2- and 6-weeks post-transplantation. Scale bars represent 50  $\mu$ m. hNCAM: human neuronal cell adhesion molecule.

In conclusion, transplantation of H9-hESC in immune-competent hosts evoked high immune reaction mediated through activation of the innate immune response (e.g., microglia activation) and the adaptive immune response (e.g., T killer cells activation). Also, as predicted the intensity of the immune response against the xenotransplant decreased over the time.

#### 4.2. Injection of CMV-GFP and CBA-GFP AAV vectors did not provide information about time-dependent expression

The biggest obstacle in our study was to determine the shortest time window for the expression of the virus, mediated by either CMV or CBA



promoter. As described in the Materials and Methods, one rat was injected i.m. bilaterally (left–right) with CMV-GFP or CBA-GFP AAV vectors (Figure 2A-B), respectively. To assess the expression of the virus, the animal was sacrificed five days after the injection. After perfusion, tissue from the *vastus intermedius* muscle from both legs was collected. For easier handling, the muscle samples were embedded in paraffin. Both samples were then assessed using IHC and PCR techniques. Initially, sections were stained with anti-GFP primary and fluorophore–conjugated secondary antibody to increase the intensity of the GFP signal. In either case, it was not distinguishable whether the detected green fluorescence was the signal coming from the expression of the GFP (Figure 5A-B). In the paper published by Jackson et al. (39) green autofluorescence, resembling fluorescent expression of GFP was observed in skeletal tissue of mice. Based on these results, we could not validate time–dependent expression of either promoter solely based on the immunofluorescent staining.

To further investigate time–dependent expression of promoters, we performed PCR and DNA electrophoresis on an agarose gel. Firstly, RNA was extracted from paraffin-embedded samples as described. After RNA extraction, concentrations of CMV AAV vector and CBA AAV vectors were 32 ng/μl and 29 ng/μl, respectively. Following RNA extraction, 300 ng of total RNA from our samples was retrotranscribed in cDNA. To analyse the expression of promoters, we did PCR and DNA electrophoresis. We used the specific forward and reverse primers for the GFP and GAPDH genes (Table 2). In the first attempt (Figure 5C) we got an inconclusive result. On the one hand, we could see positive bands, corresponding to the size of the PCR fragment (118 bp) for the housekeeping gene; GAPDH. However, regarding GFP, the bands present on the agarose gel were very faint, but the size of the bands was equivalent to the predicted size of the GFP PCR product (379 bp). To obtain stronger bands, we repeated the PCR by increasing the number of amplification cycles.



The results of that PCR are shown in Figure 5D. Unfortunately, the negative control in the amplification of the GFP gene produced a very strong band, unlike the negative control for the housekeeping gene. A possible answer to these results could be GFP contamination, very often present when working with GFP. To analyse the possible source of the contamination, we performed multiple PCR and DNA electrophoresis analysis (data not shown) altering buffers, but we did not determine the cause. Taking all the presented results into consideration, we could not say whether either one of the tested promoters can provide short time-dependent expression.

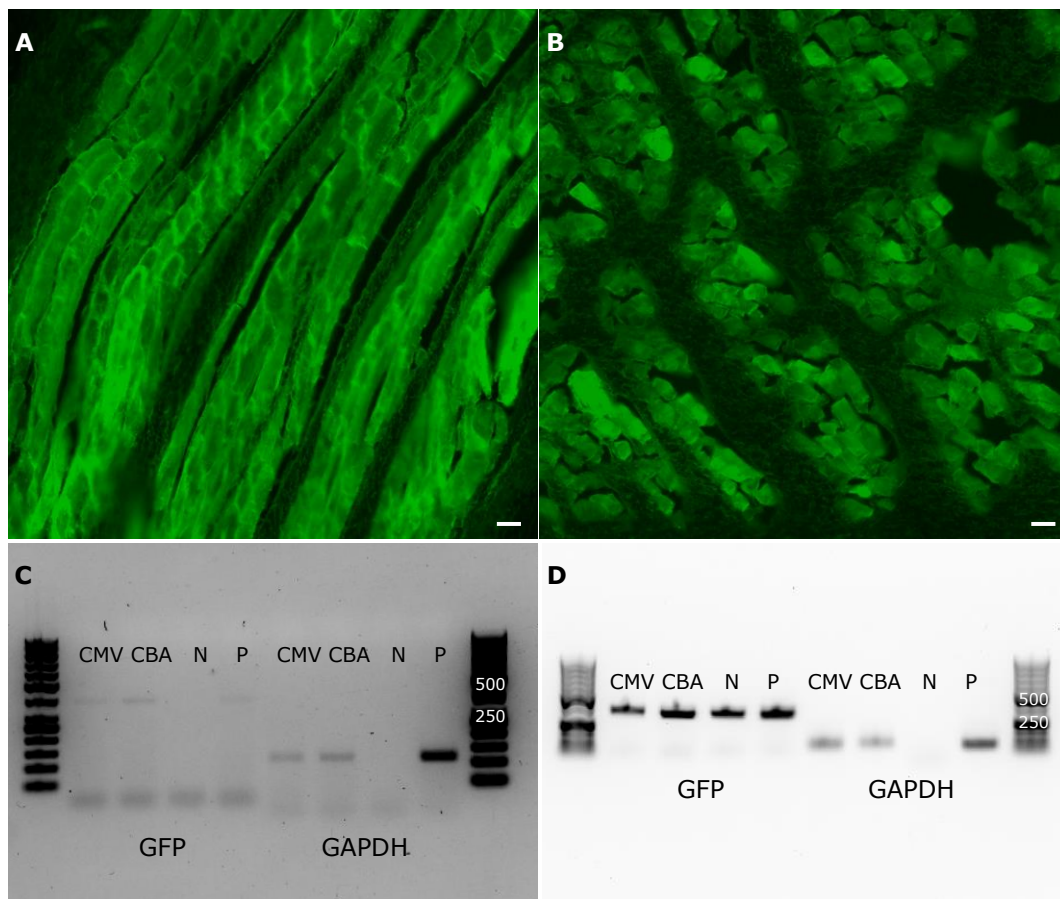


**Figure 5 CMV-GFP and CBA-GFP AAV vectors did not express GFP in five days.** Representative image of the muscle section injected with CMV-GFP (A) and CBA-GFP (B) construct, after immunofluorescent staining against GFP. Magnification 20x, scale bars represent 50  $\mu$ m. Images of the agarose gel after performing PCR with 25 amplification cycles (C) and 35 amplification cycles (D). The size of the ladder fragments is indicated in bp. Cytomegalovirus promoter(CMV), Cytomegalovirus  $\beta$ -actin promoter (CBA), Green fluorescent protein (GFP), Glyceraldehyde 3-phosphate dehydrogenase (GAPDH), negative (N), positive(P).



### 4.3. Injection of CBA-aSyn AAV vector provided sufficient information about time-dependent expression

In the second attempt to assess time-dependent expression, we injected a new viral construct. The animal was injected i.m. unilaterally with a CBA-aSyn AAV vector (Figure 2C). To assess the expression of the virus, the animal was sacrificed five days after the injection. After perfusion, tissue from the *gastrocnemius* was collected, followed by the paraffin embedding process. The assessment of the expression was done with IHC and PCR methods. Firstly, the tissue was stained with anti-aSyn primary and fluorophore-conjugated secondary antibody. To avoid green autofluorescence of the muscle tissue, samples were visualized in the red part of the electromagnetic spectra. Besides anti-aSyn, the sections were stained with fluorescent dye DAPI, to see possible colocalization. Since in this case the virus was injected unilateral, to look at the diffusion ability of the virus we also analysed the muscle tissue from the other non-injected muscle. When imagining the tissue from the injected leg, we noticed possible viral expression (Figure 6A) which was colocalized in the nucleus of the cell (Figure 6A'', white circle). The same was not seen in the muscle samples from the non-injected leg (Figure 6B'') or from the control animal (Figure C''). However, we could not guarantee if our finding was coming from the viral expression of aSyn or background noise.

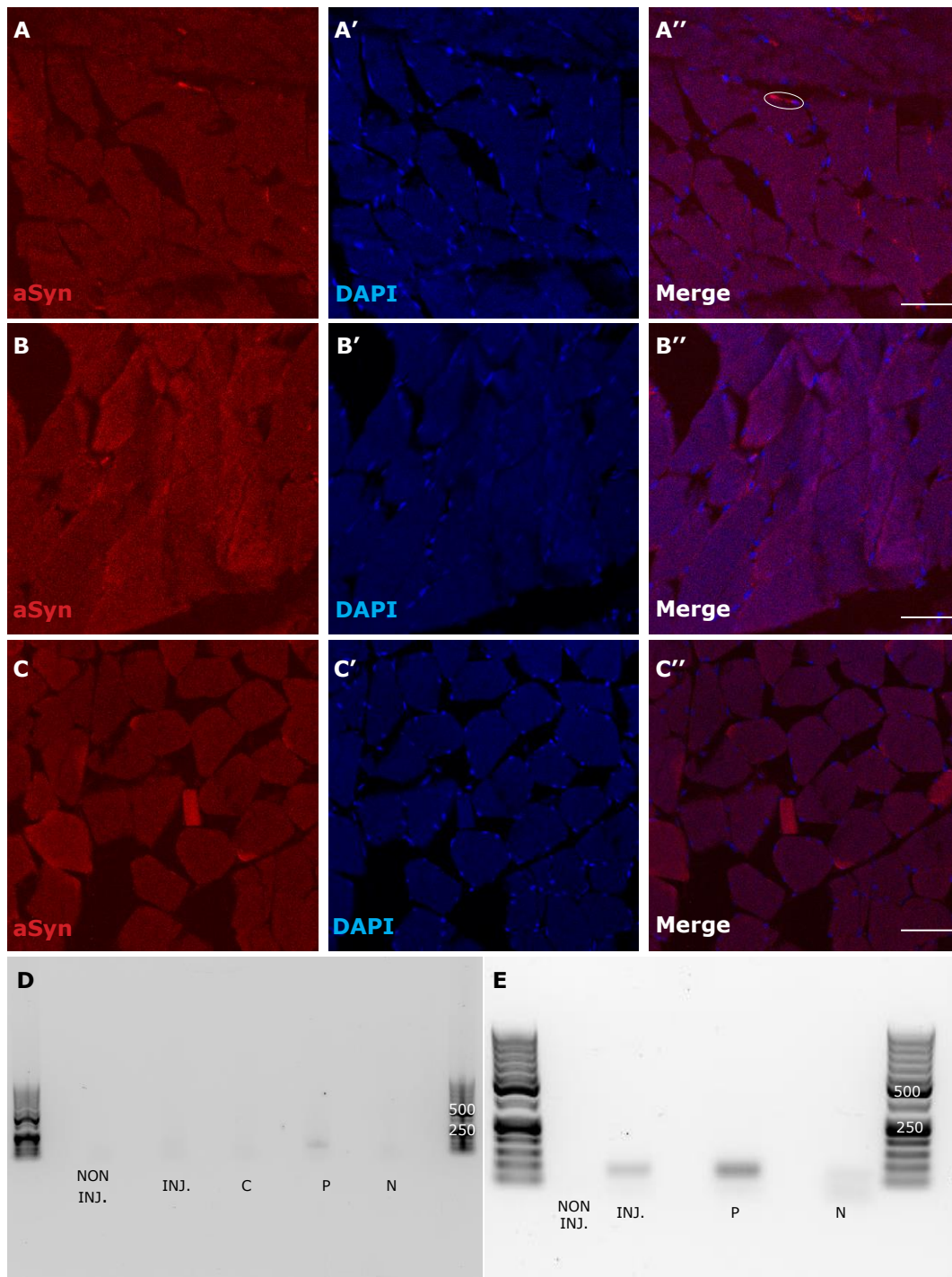


**Figure 6 Expression of CBA-aSyn AAV vector was noticeable 5 days post injection.** Representative images of the immunofluorescent labelling of human aSyn and DAPI in injected (A-A''), non-injected (B-B'') and control muscle tissue (C-C''). White circle indicates possible colocalization. Scale bars represent 50  $\mu$ m. Images of the agarose gel after PCR amplification of human aSyn with haSyn\_A primers (D) and haSyn\_J primers (E). The size of the ladder fragments is indicated in bp. aSyn(human  $\alpha$ -synuclein protein), non-injected(non inj.), injected(inj.), control (C), positive (P), negative (N).



Subsequently, we performed PCR and DNA electrophoresis to determine if indeed we have viral expression. Firstly, RNA was extracted from the paraffin-embedded samples, as described, giving the following concentrations: 23 ng/ $\mu$ l, 12 ng/ $\mu$ l, and 14 ng/ $\mu$ l from the injected, non-injected and control sample, respectively. After, 300 ng of the total RNA was retrotranscribed into cDNA and amplified with PCR. PCR reactions were carried out in two different rounds with a specific set of primers (Table 2). In the first PCR reaction, the human aSyn gene was amplified using haSyn\_A set of primers, while in the second PCR reaction we used haSyn\_J set of primers. In the first case, we used set of primers with overhangs, amplifying the PCR product size of 398 bp. After visualizing the agarose gel, we could not see bands corresponding to the size of the PCR product from any of the samples (Figure 6D). PCR of the samples was then repeated, but with a different set of primers that amplify the PCR product size of 79 bp. In this case, we saw a positive band matching the predicted size of the PCR fragment (Figure 6E). However, a faint band in the negative control were also observed, although we believe that the band was not matching the size of the predicted PCR product.

Even though the results presented were inconclusive, we hypothesized that the time - dependent viral expression is achievable by using CBA promoter.

#### 4.4. Construction and validation of the CBA-HLA class I AAV vectors

Based on the obtained results, the backbone of the pCBA-aSyn (Figure 2C) vector was chosen as a primary construct in our study. The first step in the cloning of three HLA class I molecules was to obtain a linear backbone structure. To achieve that, CBA-aSyn plasmid was digested with the NotI restriction enzyme (Figure 2C'). In total 1  $\mu$ g of the plasmid was digested. Since the digestion was performed with only one restriction enzyme, to prevent self-ligation of the digested backbone, the NotI cut sites were



dephosphorylated. After digestion, DNA was separated by electrophoresis on 1% agarose gel. Two strong bands were visible around the size predicted for the size of the digested backbone (5389 bp) (Figure 7A), indicating that the digestion was successful. Furthermore, two smaller bands were noticed that correspond to the size of the cut aSyn insert (431 bp) (Figure 7A). Given all these results, we confirmed the successful digestion of the CBA-aSyn plasmid. Afterwards, the bands equivalent to the size of the digested backbone were excised and recovered from the gel, yielding a concentration of 52 ng/ $\mu$ l.

The open reading frame (ORF) of the sequenced inserts of HLA-A, HLA-B and HLA-C specific alleles (GenScript) were amplified with a specific set of primers (Table 2). The designed primers were furthered with the addition of the NotI restriction enzyme site and three base pairs. PCR was set up as described in Materials and Methods, with the melting temperature matching the melting temperature of the specific primers (Table 2). After the amplification, the inserts were separated with DNA electrophoresis and visualized. In all three instances, amplification of the inserts produced strong bands with size matching to the expected size of each insert (Figure 7B). The sizes of the products were as follows: 1120 bp, 1111 bp, and 1123 bp for the HLA-A, HLA-B, and HLA-C fragments, respectively. Following the DNA electrophoresis on the agarose gel, the fragments were excised from the gel and recovered. The concentrations of the inserts were: 119 ng/ $\mu$ l, 102 ng/ $\mu$ l, and 186 ng/ $\mu$ l for the HLA-A, HLA-B, and HLA-C fragments, respectively.

Another step before ligation of the inserts and the digested backbone was the digestion and phosphorylation of the amplified inserts. Again, we used the NotI restriction enzyme in the digestion of the inserts, following the already described procedure. Immediately after digestion, the fragments were phosphorylated as it was described above. To validate the digestion,



inserts were separated with DNA electrophoresis. After the visualization of the agarose gel, we observed three strong bands, matching the expected size of the fragments (Figure 7C). The expected sizes of the digested fragments were: 1098 bp, 1089 bp, and 1101 bp for the HLA-A, HLA-B, and HLA-C inserts, respectively. After excision and DNA recovery from the agarose gel, the concentrations were as follows: 53 ng/ $\mu$ l, 79 ng/ $\mu$ l, and 56 ng/ $\mu$ l for the HLA-A, HLA-B, and HLA-C fragments, respectively.

Ligation and transformation of the clones and the negative control were performed as described in the Materials and Methods. The day after transformation and plating the bacteria, one colony for each clone was picked and grew again overnight in the same conditions, while the plate was stored at 4°C. The important thing to note is that in the negative control were no colonies. The following day, DNA was extracted as it was described above. The concentrations of the DNA were: 467 ng/ $\mu$ l, 1098 ng/ $\mu$ l, and 244 ng/ $\mu$ l for the pHLA-A, pHLA-B, and pHLA-C clones, respectively.

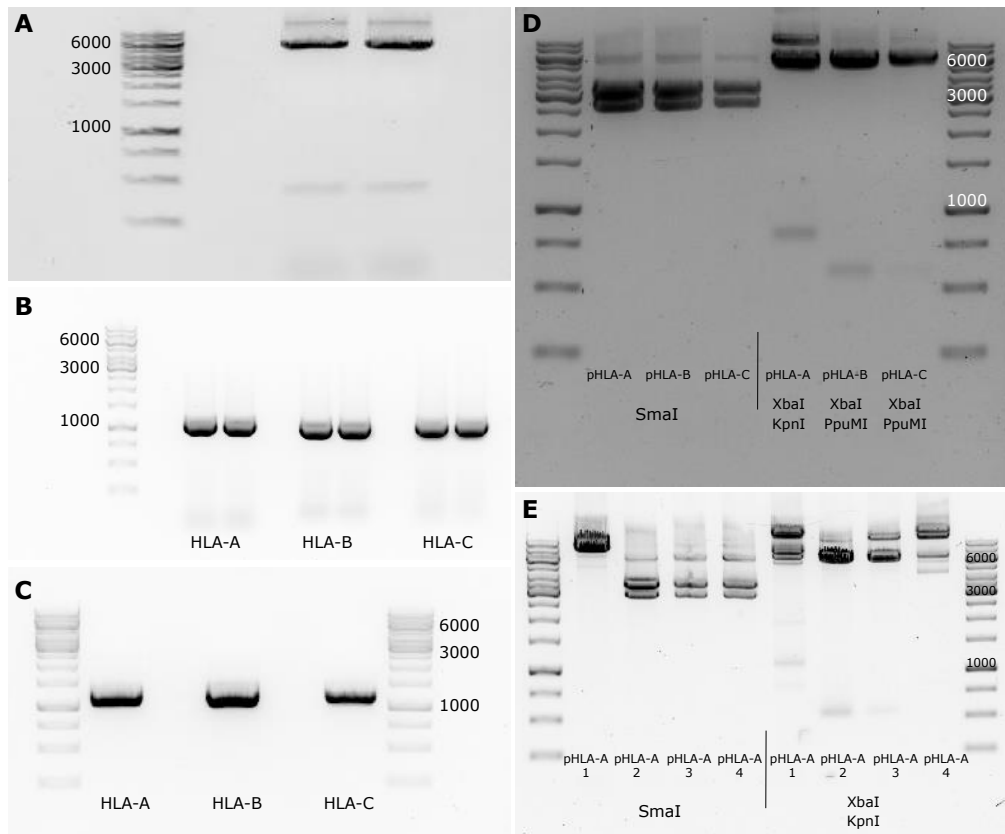


**Figure 7 Successful production of clones with specific HLA class I fragment inserts.** Digestion of the CBA-aSyn plasmid with NotI restriction enzyme (A). PCR amplification of inserts using a NotI specific set of primers (B). Digestion of amplified PCR inserts with the NotI restriction enzyme (C). Digestions of the created plasmids (pHLA-A, pHLA-B, and pHLA-C) with SmaI and specific combination of restriction enzymes (D). Simultaneous digestions of all remaining pHLA-A colonies (n=4) with SmaI and XbaI/KpnI restriction enzymes (E). The size of the ladder fragments is indicated in bp.

Validation of the produced clones was done by performing two digestion reactions: one with SmaI restriction enzyme and the other with a combination of restriction enzymes specific for each clone. The plasmid backbone used in this study contained two Inverted Terminal Repeats (ITRs), specific for plasmids used to produce the AAV vectors. Digestion with SmaI restriction enzyme generates four fragments: two 11 bp (cannot be visualized on the gel), one 3007 bp big fragment, and one specific fragment. In our case digestion with the SmaI restriction enzyme should generate the following specific size fragments: 3466 bp, 3457 bp, and 3469 bp, for the pHLA-A, pHLA-B, and pHLA-C clones, respectively. After performing the digestion and DNA electrophoresis, we observed the bands



matching the size of the digested fragments in all three clones (Figure 7D), which confirmed the preservation of the ITRs. Further confirmation was performed with a specific combination of the restriction enzymes. For the pHLA-A clone, digestion at XbaI and KpnI restriction sites produce 539 bp, and 5956 bp fragments. Digestion at XbaI and PpuMI restriction sites for the pHLA-B and pHLA-C clones produce 587 bp fragment for either clone, and 5905 bp and 5911 bp fragments for pHLA-B and pHLA-C, respectively. After the specific digestion we noticed that in the case of the pHLA-A, the bands present on the agarose gel were not of the expected size (Figure 7D). On the other hand, digestion of the pHLA-B and pHLA-C generated bands of the anticipated size (Figure 7D), suggesting that the HLA-B and HLA-C fragments were successfully cloned into the chosen backbone.

Since the pHLA-A clone did not generate the anticipated results, we repeated the process. The remaining colonies from the agar plate (n=4) were picked and grew overnight in the same conditions. The following day DNA was extracted from the samples as it was described before. The concentrations of the DNA were: 48 ng/ $\mu$ l, 81 ng/ $\mu$ l, 153 ng/ $\mu$ l and 151 ng/ $\mu$ l for the pHLA-A1, pHLA-A2, pHLA-A3 and pHLA-A4 clones, respectively. For the validation of the clones, the same digestion set-up was performed. In the case of perseverance of the ITRs validated through SmaI digestion, all clones, except pHLA-A1, produced bands of the expected size (Figure 7E). Furthermore, digestion with XbaI and KpnI restriction enzymes generated the bands of the predicted size only in the case of the pHLA-A2 and pHLA-A3 clones (Figure 7E). Taking these results together, we can say that pHLA-A2 and pHLA-A3 clones contain the desired sequence and can be used in the further step of the viral production. In conclusion, the desired HLA class I molecules were successfully cloned into the chosen backbone. The produced clones can be used in the next stages of the project, which include the production of the AAV vectors.



## 5. Discussion

Transplantation of the differentiated hESC is a strong asset in the treatment of PD. Although hESCs are less immunogenic than adult cells (37), transplantation and long term assessment in animal models of PD requires some form of immunosuppressive intervention. Current methods include the usage of immunosuppressant drugs (e.g., CsA) or immune-deficient animals. The former has the disadvantage that repeated administration of the immunosuppressive agent can only be administered for a limited amount of time (<20 weeks), which can limit the study to immature neurons whereas the latter approach does allow for long term graft survival but limits the behavioural assessment as the barrier environment cannot be breached.

An alternative novel method is based on the neonatal desensitization of the animals, which surpasses the problem of long term immunosuppression, and allows prolonged survival of the transplant in fully immune-competent hosts (28). The big emphasis in neonatal desensitization is the short time frame in which the host's immune system can be adapted to the human antigens presented on the hESC. Currently, animals desensitized up to 5 days after birth, have been shown to have reduced immune response and longer survival rate of the transplant (28,30). Now, neonatal desensitization is accomplished by injection of the cell suspension in the neonates.

However, many factors on how this desensitization is achieved remain elusive. Successful approaches have been demonstrated in SD rats using a mix of differentiated and undifferentiated hESCs as well as primary foetal tissue, whereas other rat strains and undifferentiated cells have not succeeded. No success has yet been reported using the neonatal desensitisation approach in mice. Previously published results suggest that differentiated cells possess some surface markers that are imperative for the procedure to succeed. Furthermore, the time during which the adaptive



immune system is malleable seems to be limited and different between species. In the seminal studies by Billingham (26) for example, mice were already inoculated *in utero* whereas in SD rats this has been reported to work up to post-natal day 5. One limiting factor in the widespread implementation of neonatal desensitisation is the required timing of the birth of the pups with the differentiation of the donor cells. An off-the-shelf approach would facilitate the usage of this model. Furthermore, the mechanism by which neonatal desensitisation is induced remains elusive. Using differentiated cells, we cannot investigate which aspect of the cell suspension we inject is essential. Therefore, in our study, we opted for a more specific induction of neonatal desensitization, mediated by inoculation of AAV vectors in rat pups. This approach has the advantage that the AAV vectors can be prepared, stored, and injected on demand. Furthermore, if successful, it can be used to single out individual transgenes which are essential in the conferring of immune tolerance.

Our first goal was to identify the surface antigens present on the H9 hESC line, and creating a library of clones with those specific genes. Since the first isolation of the H9 line (31), this cell line was highly studied and characterized. Differentiated H9 hESC express both HLA class I and HLA class II molecules, but the expression differs when compared to the undifferentiated H9 hESC (40). We identified three HLA class I alleles: HLA-A 03:01, HLA-B 07:02 and HLA-C 07:01, and sequenced the coding sequence (GenScript) of each allele.

As mentioned before, a critical point in the achievement of neonatal desensitization is the short time window in which the host's immune system can be adapted to presented antigens. Therefore, we tried to validate the expression of the virus with injections of three different constructs. Firstly, we injected two different AAV vectors carrying the gene for GFP. One virus was expressed through the CMV promoter, while the other virus was expressed by the CBA promoter. CMV promoter and hybrid CBA promoters



generally provide strong, long term expression and are commonly used in gene transfer studies (41). In both cases, our results did not provide enough information about time-dependent expression of the virus. The first major drawback of this optimization step was the inability to distinguish the fluorescence of the GFP from the autofluorescence of the sample. As it has been reported (39), skeletal muscle tissue gives green autofluorescence that resembles fluorescence from GFP. Therefore, we opted for the second method of validation which was PCR and DNA electrophoresis. Unfortunately, our results did not provide adequate information about the time-dependent viral expression. The big problem in this way of the assessment was contamination with GFP, because of which we had varied results and could not draw out a conclusion.

To surpass this problem, we injected a third viral construct expressing the human aSyn protein and which expression was mediated via CBA promoter. We did not observe strong expression by either mode of assessment, suggesting that the protein expression might have been too low at these early time points to be visualized. A possible option for having inconclusive results in both validation parts was the poor choice of the methods used for the assessment of the expression. Techniques like Western Blot and qPCR could have been a better choice. However, in the paper published by Huang et al. (42) viral expression mediated through CBA promoter in skeletal muscle yielded higher expression when compared to the CMV promoter vector 5 days after the injection. Therefore, we hypothesized that CBA promoter-based vector can be used for the time-dependent viral expression.

After validation of CBA based promoter vector as a feasible construct to achieve time-dependent expression, we cloned the desired inserts of HLA-A, HLA-B, and HLA-C alleles. We successfully cloned the desired sequences into the chosen backbone and created the library of clones that can be used in the next stages of the project. However, slight weakness in the cloning



process was the low number of bacterial colonies present, which were not carrying the same sequence as it was shown for the pHLA-A. We noticed that only two out of five colonies of pHLA-A were carrying the right sequence, suggesting that the possible problem was in the bacteria used for the transformation. Because of this, sequencing of the clones would be next step for the complete validation of the successful cloning. Nevertheless, we have confirmed that we have successfully cloned and created plasmids carrying the wanted sequence.

Following the successful creation of three clones, we accomplished the first step in the AAV vector-based neonatal desensitization. Besides these clones, a library containing other surface markers found on H9 hESC could be created in the future. The next steps would include the production of the AAV vectors and the desensitization of the animals, followed by the chemical induction of PD and transplantation. Time-dependent viral expression could also be evaluated following the neonatal desensitization. Altogether, our results suggest that neonatal desensitization based on the injection of the AAV vectors could be a reasonable method in the assessment of cell replacement therapy for PD.



## 6. Conclusion

For the accomplishment of AAV vector-based neonatal desensitization, we established a library of clones carrying the sequence for three different HLA class I alleles. Clones that we constructed are based on CBA promoter, which has been shown to yield a high expression in muscle cells after only 5 days post-injection (42). Unfortunately, our results in the validation of CBA promoter did not provide enough evidence for time-dependent expression, suggesting the inadequate choice of techniques used for the assessment. Additionally, validation of CMV promoter-based vector was not achieved, due to the possible green autofluorescence of the muscle tissue that strongly resembles the fluorescence of GFP (39). Nevertheless, we have successfully created pHLA-A, pHLA-B, and pHLA-C clones, which can be used for the next step in this project.



## 7. Literature

1. Tysnes OB, Storstein A. Epidemiology of Parkinson's disease. *J Neural Transm.* 2017;124(8):901–5.
2. Parkinson J. An essay on the Shaking Palsy. *Arch Neurol.* 1969;20(4):441–5.
3. Darden W, Przedborski S. Parkinson's Disease: Mechanisms and Models. *Neuron.* 2003;39:889–909.
4. Jankovic J. Parkinson's disease: Clinical features and diagnosis. *J Neurol Neurosurg Psychiatry.* 2008;79(4):368–76.
5. Moustafa AA, Chakravarthy S, Phillips JR, Gupta A, Keri S, Polner B, et al. Motor symptoms in Parkinson's disease: A unified framework. *Neurosci Biobehav Rev.* 2016;68:727–40.
6. Ball N, Teo WP, Chandra S, Chapman J. Parkinson's disease and the environment. *Front Neurol.* 2019;10(March):218–26.
7. Braak H, Del Tredici K. *Neuroanatomy and Pathology of Sporadic Parkinson's disease.* Springer. 2009. 1–89 p.
8. Schulz JB, Falkenburger BH. Neuronal pathology in Parkinson's disease. *Cell Tissue Res.* 2004;318(1):135–47.
9. Franco R, Reyes-Resina I, Navarro G. Dopamine in health and disease: Much more than a neurotransmitter. *Biomedicines.* 2021;9(2):1–13.
10. Goedert M. Alpha-Synuclein and Neurodegenerative Diseases. *Nature.* 2001;2(July):492–501.
11. Jenco JM, Rawlingson A, Daniels B, Morris AJ. Regulation of phospholipase D2: Selective inhibition of mammalian phospholipase D isoenzymes by  $\alpha$ - and  $\beta$ -synucleins. *Biochemistry.* 1998;37(14):4901–9.
12. Bendor JT, Logan TP, Edwards RH. The function of  $\alpha$ -synuclein. *Neuron.* 2013;79(6):1044–66.
13. Polymeropoulos MH, Lavedan C, Leroy E, Ide SE, Dehejia A, Dutra A, et al. Mutation in the  $\alpha$ -synuclein gene identified in families with Parkinson's disease. *Science (80- ).* 1997;276(5321):2045–7.
14. Cherian A, Divya KP. Genetics of Parkinson's Disease. *Acta Neurol Belg.* 2020;10:9–33.



15. Li JQ, Tan L, Yu JT. The role of the LRRK2 gene in Parkinsonism. *Mol Neurodegener.* 2014;9:47–66.
16. Obeso JA, Rodriguez-Oroz MC, Goetz CG, Marin C, Kordower JH, Rodriguez M, et al. Missing pieces in the Parkinson's disease puzzle. *Nat Med.* 2010;16(6):653–61.
17. De Miranda BR, Castro SL, Rocha EM, Bodle CR, Johnson KE, Greenamyre JT. The industrial solvent trichloroethylene induces LRRK2 kinase activity and dopaminergic neurodegeneration in a rat model of Parkinson's disease. *Neurobiol Dis.* 2021;153(1):1–14.
18. William Langston J, Ballard P, Tetrud JW, Irwin I. Chronic parkinsonism in humans due to a product of meperidine-analog synthesis. *Science (80- ).* 1983;219(4587):979–80.
19. Betarbet R, Sherer TB, Mackenzie G, Garcia-osuna M, Panov A V, Greenamyre JT. Chronic systemic pesticide exposure produces pd symptoms Betarbet. *Nat Neurosci.* 2000;26:1301–6.
20. Hauser RA. Levodopa: Past, present, and future. *Eur Neurol.* 2009;62(1):1–8.
21. Lewitt PA. Levodopa for the Treatment of Parkinson ' s Disease. *N Engl J Med.* 2008;359(23):2468–76.
22. Hammond C, Bergman H, Brown P. Pathological synchronization in Parkinson's disease: networks, models and treatments. *Trends Neurosci.* 2007;30(7):357–64.
23. Lindvall O, Björklund A. Cell Therapy in Parkinson's Disease. *NeuroRx.* 2004;1(4):382–93.
24. Li JY, Englund E, Holton JL, Soulet D, Hagell P, Lees AJ, et al. Lewy bodies in grafted neurons in subjects with Parkinson's disease suggest host-to-graft disease propagation. *Nat Med.* 2008;14(5):501–3.
25. Winkler C, Kirik D, Björklund A. Cell transplantation in Parkinson's disease: How can we make it work? *Trends Neurosci.* 2005;28(2):86–92.
26. Billingham RE, Brent L, Medawar PB. "Actively acquired tolerance" of foreign cells. *Nature.* 1953;172(4379):603–6.
27. Billingham RE, Brent L. Acquired Tolerance of Foreign Cells in Newborn Animals. *Proc R Soc London.* 1956;146(922):78–90.
28. Kelly CM, Precious S V., Scherf C, Penketh R, Amso NN, Battersby A, et al.



- Neonatal desensitization allows long-term survival of neural xenotransplants without immunosuppression. *Nat Methods*. 2009;6(4):271–3.
29. Janowski M, Jablonska A, Kozłowska H, Orukari I, Bernard S, Bulte JW, et al. Neonatal desensitization does not universally prevent xenograft rejection. *Nat Methods*. 2012;9(9):858.
  30. Heuer A, Jönsson ME, Pfisterer U, Kirkeby A, Parmar M. HESC-derived neural progenitors prevent xenograft rejection through neonatal desensitisation. *Exp Neurol*. 2016;282:78–85.
  31. Thomson JA. Embryonic stem cell lines derived from human blastocysts. *Science* (80- ). 1998;282(5391):1145–7.
  32. Löser P, Schirm J, Guhr A, Wobus AM, Kurtz A. Human embryonic stem cell lines and their use in international research. *Stem Cells*. 2010;28(2):240–6.
  33. Leone P, Shin EC, Perosa F, Vacca A, Dammacco F, Racanelli V. MHC class I antigen processing and presenting machinery: Organization, function, and defects in tumor cells. *J Natl Cancer Inst*. 2013;105(16):1172–87.
  34. Klein J, Sato A. The HLA System. *N Engl J Med*. 2000;343(10):702–9.
  35. Anaya J-M, Shoenfeld Y, Rojas-Villarraga A, Levy RA, Cervera R. Autoimmunity. 2013. 872 p.
  36. Sidney J, Peters B, Frahm N, Brander C, Sette A. HLA class I supertypes: A revised and updated classification. *BMC Immunol*. 2008;9:1–15.
  37. Drukker M, Katchman H, Katz G, Even-Tov Friedman S, Shezen E, Hornstein E, et al. Human Embryonic Stem Cells and Their Differentiated Derivatives Are Less Susceptible to Immune Rejection Than Adult Cells. *Stem Cells*. 2006;24(2):221–9.
  38. Carpenter MK, Rosler ES, Fisk GJ, Brandenberger R, Ares X, Miura T, et al. Properties of Four Human Embryonic Stem Cell Lines Maintained in a Feeder-Free Culture System. *Dev Dyn*. 2004;229(2):243–58.
  39. Gitleman L. Skeletal Muscle Fiber-Specific Green Autofluorescence: Potential for Stem Cell Engraftment Artifacts. *Pap Knowl Towar a Media Hist Doc*. 2014;
  40. Li, L.; Baroja, M.L.; Ajumdar, A.; Chadwick, K.; Rouleau, A.; Gallacher, L.; Ferber, I.; Lebkowski, J.; Martin, T.; Madrenas, J.; Bhatia M. Human Embryonic Stem Cells Possess Immune-Privileged Properties. *Stem Cells*. 2004;22(4):448–56.



41. Gray SJ, Foti SB, Schwartz JW, Bachaboina L, Taylor-Blake B, Coleman J, et al. Optimizing promoters for recombinant adeno-associated virus-mediated gene expression in the peripheral and central nervous system using self-complementary vectors. *Hum Gene Ther.* 2011;22(9):1143–53.
42. Huang J, Ito Y, Kobune M, Sasaki K, Nakamura K, Dehari H, et al. Myocardial injection of CA promoter-based plasmid mediates efficient transgene expression in rat heart. *J Gene Med [Internet].* 2003;5(10):900–8.